

The near-field method: a modified equivalent linear method for dynamic soil–structure interaction analysis. Part II: verification and example application

Hadi Sayyadpour¹ · Farhad Behnamfar¹ · M. Hesham El Naggar²

Received: 21 August 2015 / Accepted: 18 January 2016 / Published online: 25 January 2016
© Springer Science+Business Media Dordrecht 2016

Abstract Usually for modeling of soil in a direct soil–structure interaction (SSI) problem, the equivalent linear soil properties are used. However, this approach is not valid in the vicinity of a foundation, where the soil experiences large strains and a high level of nonlinearity because of structural vibrations. The near-field method was developed and described in a companion paper to overcome this limitation. This method considers the effects of large strains and suggests a shear modulus and a damping ratio further modified in the near-field of a foundation. Validity and performance of this approach are evaluated, application examples are explained and the results of a parametric study about the role of soil and structure parameters in the extent of SSI effects on the nonlinear seismic response of structures are presented in this paper. One real existing and five, ten, fifteen and twenty story moment-resisting frame steel buildings with two different site conditions corresponding to firm and soft soils are considered and the responses obtained from the near-field method are compared with the recorded and rigorous responses. Moreover, various SSI modeling techniques are employed to investigate the accuracy and performance of each approach. The results show that the near-field method is a simple yet accurate enough approach for analysis of direct SSI problems.

Keywords Soil–structure interaction · Near-field method · Nonlinear seismic response · Parametric study

✉ Farhad Behnamfar
farhad@cc.iut.ac.ir

Hadi Sayyadpour
hadisayadpour@gmail.com

¹ Department of Civil Engineering, Isfahan University of Technology, Isfahan 8415683111, Iran

² Department of Civil Engineering, The University of Western Ontario, London, ON N6A 5B9, Canada

1 Introduction

Observations after historical earthquakes have shown that soil–structure interaction (SSI) can alter the response of structures and increase the damage rate during strong ground shakings. The field of geotechnical earthquake engineering was developed after strong earthquakes of Niigata, Japan and Alaska in 1964 to investigate site and SSI effects (Bozorgnia and Bertero 2004). Various researchers developed different methods to analyze SSI effects. As a simple approach, the original SSI system can be replaced by an equivalent single degree of freedom (SDF) system with increased period and damping. This method was initially proposed in the early 1970s and nowadays is contained in building codes like ASCE 7-10 (2010). The more rigorous methods can be categorized into two main classes including the substructure and direct methods.

In the substructure method, the soil domain is replaced by appropriate elements to include soil stiffness and damping. Unlike the substructure method, the direct method includes modeling of the soil domain and the superstructure simultaneously. Although soil and structure nonlinearity can be included in the direct approach, it has some serious limitations such as how to model the unbounded soil domain and its inevitable enormous computational effort because of the many degrees of freedom in the soil domain and nonlinearity of soil. Accordingly, efforts have been made to simplify the direct method in order to make it more practical.

The equivalent linear method (ELM) is an effective method to analyze the soil–structure interaction systems. In this method, the soil behavior is assumed to be linear but the stiffness and damping properties of soil are modified to be consistent with the strain level in each layer. One of the main advantages of the ELM is its computational efficiency compared to the direct method. Cubrinovski and Ishihara (2004), Casciati and Borja (2004) and Manna and Baidya (2010) employed the ELM to solve various SSI problems. Ptilakis and Clouteau (2010) proposed an equivalent linear substructure approximation of the soil–foundation–structure interaction incorporating the effects of the primary and secondary soil nonlinearities. While the conventional ELM highly simplifies the SSI analysis, it can be in large errors in the vicinity of foundation, where the strain level in strong earthquakes is over 1 % (Ishihara 1996). Besides, the traditional ELM uses modified properties calculated through a free-field analysis and therefore, the effects of these large strains arising from inertial SSI are excluded. However, this fact is often ignored and the ELM is used for the total soil medium.

On the other hand, it can be perceived that just a limited zone in the vicinity of foundation experiences considerable nonlinear deformations. Therefore, the soil domain can be divided into two zones: the one near the foundation with nonlinear behavior (the near-field zone) and the remaining unbounded elastic part (the far-field zone) (Wolf and Song 1996).

In a recently published paper, Ghandil and Behnamfar (2015) resolved the ELM limitations and proposed the near-field method as a modified ELM with a further reduction of the soil shear modulus in the near-field zone that resulted in validity of using the ELM throughout. The present study generalizes this new approach such that it can be applicable for a wide range of structures and includes the effects of different vibrational modes of the structure. In the first part of this paper (the companion paper), a set of dimensionless parameters representing the relative properties of structure and soil including the stiffness ratio (\bar{s}), the slenderness ratio (\bar{h}) and the mass ratio (\bar{m}) were selected and a comprehensive parametric study was carried out to determine the

near-field zone dimensions and dynamic properties. Then, semi-analytical relations were proposed as functions of the dimensionless parameters to calculate the near-field properties.

Evaluating the validity and performance of the near-field method, and comparing the performance of the near-field method with other modeling approaches are the main objectives of the present paper. To attain this goal, two sets of 3D examples are considered and the open source software Open System for Earthquake Engineering Simulation (OpenSees) (Mckenna 1997; Mazzoni et al. 2007) is used to analyze different systems of this study. The first set of examples is selected from ATC-83 report (2012) and includes applying certain SSI models to an existing building and comparing with actual observed responses. In the second set of examples, a parametric study is performed with evaluating the nonlinear seismic response of five, ten, fifteen and twenty story moment-resisting frame steel buildings. Two site conditions corresponding to site classes C and E based on the ASCE 7-10 (2010) criteria along with different SSI modeling techniques are considered for this part of study. It should be noted that a nonlinear Winkler model developed by El Ganainy and El Naggar (2009) is also applied for both sets of examples to compare performance of the near-field method with another new SSI modeling technique.

More details about the employed SSI modeling techniques, the considered examples, utilizing the near-field method for each example and results of analyses are provided in the following sections.

2 The employed SSI analysis techniques

The near-field method, the rigorous method (utilizing an elastic–plastic constitutive model for the whole soil medium) and the nonlinear Winkler model are the three analysis approaches to be taken in the rest of this study. In the near-field method, as shown in the companion paper, a procedure was devised to correct the mechanical properties of soil in the vicinity of foundation due to structural vibrations. This method, proposed in this research, makes it possible to perform an equivalent linear analysis of the whole soil medium including the modified near-field properties. The meshing of the soil medium for the rigorous analysis, the boundary conditions, and selection of the time step were described in the companion paper along with the description of the near-field and rigorous methods. The Winkler method is described in this section.

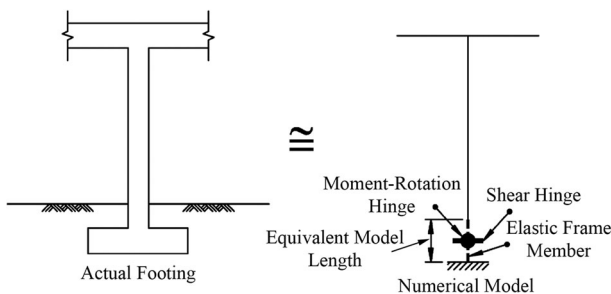


Fig. 1 The nonlinear Winkler model proposed by El Ganainy and El Naggar (2009)

2.1 The nonlinear Winkler model

The nonlinear Winkler model proposed by El Ganainy and El Naggar (2009) is used for comparison with the performance of the near-field method. In the mentioned work, an efficient 3D nonlinear Winkler model for simulating shallow foundations has been presented. This model represents the foundation in a compact assembly of three structural elements. This assembly consists of a rotation hinge, a shear hinge and an elastic frame element. Appropriate bounding surfaces are defined in this model to consider the interaction between the vertical load and biaxial moments ($P - M_B - M_L$) as well as biaxial horizontal loading condition ($V_B - V_L$). Figure 1 illustrates this nonlinear Winkler model (El Ganainy and El Naggar 2009).

The procedure outlined by El Ganainy and El Naggar (2009) is used in the current paper to calculate the mechanical and geometrical properties of the bending and shear hinges and the elastic frame member. Based on this procedure, the elastic translational stiffness and the subgrade modulus of the foundation should be calculated by available classic relations and a minimum possible length together with an appropriate cross sectional area should be assumed for the elastic frame member. Then, one can easily calculate other properties of the model using the relations provided in reference (El Ganainy and El Naggar 2009). In the following section, examples of application of the developed near-field method are presented.

3 Sherman Oaks building example

3.1 Building and site description

ATC-83 (2012) has presented two example applications analyzed with conventional soil–structure interaction modeling techniques. In this paper, one of the two, called the Sherman Oaks commercial building, has been selected to investigate the ability of the near-field method. Sherman Oaks building is a 13-story reinforced concrete moment frame structure

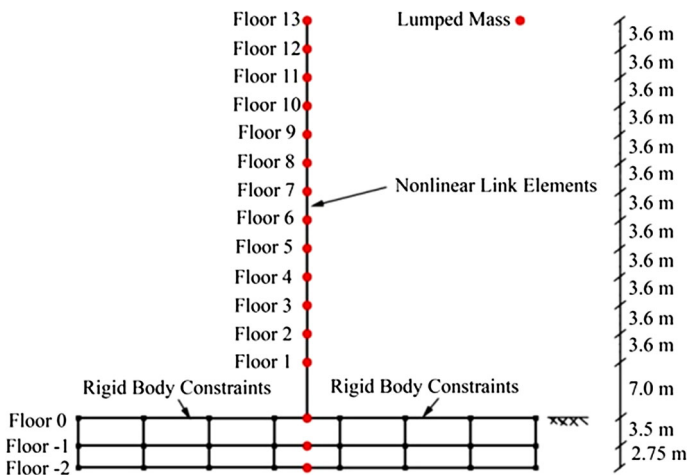


Fig. 2 Elevation view of the stick model of the Sherman Oaks building

with two basement levels, located in Sherman Oaks, California. The building measures 50 m tall from the ground surface to the roof and the plan dimensions are 21.9 m wide by 57.6 m long. The bedrock level is at depths ranging from 21 to 27 m. The average shear wave velocity for the top 30 m of the soil profile and for the soil near the foundation are equal to 320 and 200 m/s, respectively, and the average moist unit weight is taken to be 20 kN/m^3 (2012).

This building was instrumented in 1977 and six earthquake events have been recorded until now among which Northridge, Landers and Whittier events were chosen in this study. As there is no free-field instrument in the vicinity of the building, the foundation input motion (\ddot{u}_{FIM}) was used as input motion in free-field analysis of the site.

A full and a stick model have been utilized by ATC-83 for the Sherman Oaks building. Since no enough details have been provided to model the full structure in this study, here the structure is idealized as a stick model and the periods are compared with those of the full model analysis presented in ATC-83. The stick model of the building is illustrated in Fig. 2.

Stiffness properties of each floor above ground surface are modeled by an equivalent nonlinear link element having an idealized force–displacement behavior obtained from pushover analyses of that floor in the full model. For instance, Fig. 3 shows the idealized force–displacement curve for floor 11 in East–West (EW) direction as presented in ATC-83 report (2012). More details about the stick model including its lumped masses, stiffness, etc. can be found in ATC-83 (2012).

Table 1 compares the periods of the first and second translational modes of the stick model developed in this study with those of the full model of ATC-83.

3.2 Employing the near-field method

This section explains the main steps of the near-field method. The soil domain is divided into near and far-field regions. The shear modulus and damping ratio resulted from free-

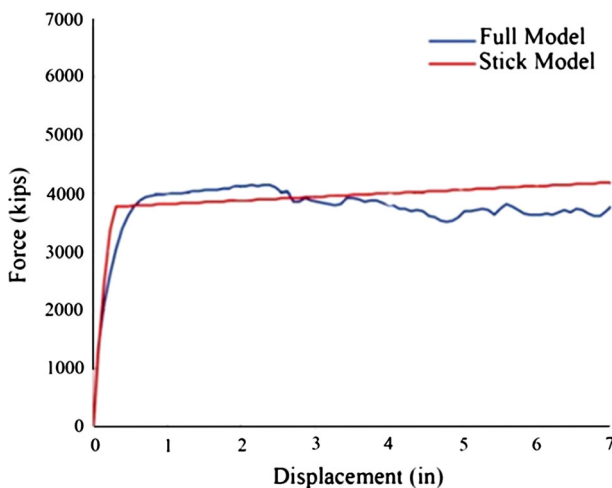


Fig. 3 Idealized force–displacement curve for floor 11 in EW direction

Table 1 Comparison of periods of the models (s)

Structural model	First mode (translational)	Second mode (rotational)	Third mode (translational)
Full (ATC-83)	2.45	2.31	2.21
Stick (this study)	2.44	–	2.19

field analysis are used in the far-field part and the near-field properties are calculated as follows.

3.2.1 Modal analysis of the fixed-base structure

The results of modal analysis of the fixed-base structure are presented in Table 2.

3.2.2 Determining the important modes

Important modes are the modes with a more contribution to the total structural response. According to Table 2 it is clear that the first three modes in each direction are enough to compute the structural responses with an acceptable accuracy.

3.2.3 Calculating dimensionless parameters for the important modes

In the near-field method semi-analytical relations are proposed to calculate geometrical and mechanical properties of the near-field region. These relations are functions of three dimensionless parameters: slenderness ratio (\bar{h}), stiffness ratio (\bar{s}) and mass ratio (\bar{m}), which control inertial SSI effects in the near-field and can be calculated as follows:

$$\bar{s} = \frac{\omega_S h}{V_S} \quad (1)$$

$$\bar{h} = \frac{h}{a} \quad (2)$$

$$\bar{m} = \frac{m}{\rho_S a^2 h} \quad (3)$$

where h refers to structure height, m is the effective modal mass of structure, V_S and ρ_S are the shear wave velocity and mass density of the soil, a is a characteristic length of the foundation (i.e. half-width or radius of the foundation) and ω_S refers to structure's angular

Table 2 Modal characteristics of the fixed-base structure

Mode	Description	Period (s)	Frequency (rad/s)	Modal participation mass ratio
1	First mode (N–S)	2.437	2.541	0.84
2	First mode (E–W)	2.202	2.854	0.86
3	Second mode (N–S)	0.839	7.485	0.10
4	Second mode (E–W)	0.752	8.360	0.095
5	Third mode (N–S)	0.501	12.531	0.030
6	Third mode (E–W)	0.449	14	0.026

frequency. The modal mass, frequency, and height are the modal analysis outputs. It should be noted that in the near-field method, the shear wave velocity of soil in the vicinity of foundation (i.e. 200 m/s) is used to calculate the stiffness ratio \bar{s} . Table 3 shows the dimensionless parameters $\bar{h}, \bar{s}, \bar{m}$ calculated for the first three modes of the fixed-base structure.

3.2.4 Calculating the shear modulus modification factor and damping ratio of the near-field region for important modes

Equations 4 and 5 (repeating Eqs. 15, 16 of the companion paper) are used to calculate the shear modulus modification factor and damping ratio of the near-field region and Table 4 illustrates these values for important modes.

$$\frac{G_{Near-Field}}{G_{Free-Field}} = \frac{0.6}{\left(\frac{\bar{s}^{1.5} \times \bar{m}^{0.10}}{\bar{h}^{0.25}}\right) + 0.6} \tag{4}$$

$$\xi = 18 \left(\frac{\bar{s}^{1.5} \times \bar{m}^{0.10}}{\bar{h}^{0.25}}\right) + 3 \tag{5}$$

3.2.5 Computing weighted average of the shear modulus modification factor and damping ratio

The mass participation factor of each mode is considered as a weight and the values mentioned in Table 5 are obtained after computing the weighted average of the near-field properties.

Should the analysis have been done under two simultaneous horizontal components of ground motion, the minimum value of shear modulus modification factors and the maximum value of damping ratios in two directions would be used as near-field properties.

3.2.6 Computing the near-field dimensions in each direction

Plan dimensions and thickness of the near-field zone are calculated using Eqs. 17 and 18 of the companion paper. The resulting values are presented in Table 6.

3.3 Nonlinear time history analysis of the Sherman Oaks building

The near-field method has the great advantage that with using the modified properties, behavior of the soil medium can be taken as being linear both in the near and far-field

Table 3 Dimensionless parameters for the important modes

Mode	Description	\bar{h}	\bar{m}	\bar{s}
1	First mode (N–S)	3.192	0.142	0.445
2	First mode (E–W)	1.198	0.147	0.492
3	Second mode (N–S)	0.488	0.110	0.20
4	Second mode (E–W)	0.292	0.066	0.352
5	Third mode (N–S)	0.743	0.023	0.511
6	Third mode (E–W)	0.253	0.021	0.511

Table 4 Shear modulus modification factor and damping ratio of the near-field region

Mode	Description	$G/G_{Free-Field}$	ζ (%)
1	First mode (N–S)	0.77	6.3
2	First mode (E–W)	0.69	7.9
3	Second mode (N–S)	0.88	4.5
4	Second mode (E–W)	0.73	6.9
5	Third mode (N–S)	0.69	7.8
6	Third mode (E–W)	0.63	9.3

Table 5 Shear modulus modification factors and damping ratios of the near-field zone for the Sherman Oaks building

Direction	$G/G_{Free-Field}$	ζ (%)
Longitudinal (E–W)	0.68	7.7
Transverse (N–S)	0.76	6.0

regions. This ability saves a large portion of the computing time. Meanwhile, the structure can in general behave nonlinearly in this method as is the assumption in this example. For comparison, the conventional ELM (i.e. $G = G_{Free-Field}$) and the El Ganainy-El Naggar's nonlinear Winkler approach are adopted herein in separate modeling and analyses of the same problem. A one-dimensional free-field site response analysis is conducted for each earthquake to compute the far-field properties and the ground motion at the bedrock level. The ground motions at the bedrock and base levels are input to the near-field and Winkler models, respectively.

The relative difference of the results of El Ganainy's model, the near-field method and the conventional ELM with regard to the observed responses of the building are presented in the following under the mentioned earthquakes. The responses are represented at floor levels $-2, 0, 1, 7$ and 13 where the recorded responses are available (Figs. 4, 5, 6).

Results of the above analyses show that application of the near-field method to the Sherman Oaks building example has led to a very good accuracy. It can be seen that employing the near-field method improves the performance of the conventional ELM. In most cases the accuracy is superior to the El Ganainy's method. ATC-83 (2012) has presented the results of analysis of this building with other conventional modeling approaches including with springs and dashpots concentrated at the base (the substructure approach). Comparison of the results of this study with those of ATC-83 (2012) reveals that, in the case of the Sherman Oaks building, the near-field (and the El Ganainy's) methods are much more accurate than the substructure method.

Table 6 Near-field dimensions for the Sherman Oaks building

Direction	Partial length from Eq. 17 of the companion paper ($L_{N.F.}/2a$)	Total length ($2L_{N.F.} + 2a$) (m)	Depth ($H_{N.F.}$) (m)
Longitudinal (E–W)	0.415	95	8.89
Transverse (N–S)	0.371	38	8.89

4 Steel moment resisting frame buildings

Extending the performance evaluation of the near-field method to a wide range of examples is the main purpose of this part of the study. For this purpose, 3D nonlinear time history analyses are conducted for several moment-resisting steel structures having five to twenty stories. Two site classes are considered for the underlying soil medium and various modeling techniques are adopted to analyze comparatively the soil–structure interaction effects on the buildings.

4.1 Description of the buildings

4.1.1 Geometry and the structural system

Four buildings with 5, 10, 15 and 20 stories are selected. The buildings have similar plans with 6×5 bays spanning 6 m unanimously in each bay and a constant story height of 3.5 m. Two-way steel moment-resisting frames are considered as the lateral resisting system of the buildings. The floor system consists of concrete slabs having a thickness of 0.2 m. The slabs are assumed to be rigid in plane.

4.1.2 Gravity loads

The gravity loads assigned to the buildings consist of the self weight of structural and nonstructural components (partitions) as well as the live load carried on the floors. The unit weights and the imposed loads are summarized in Table 7.

4.1.3 Material specifications

Tables 8 and 9 list the properties of the steel and concrete materials for the structural members and foundations, respectively.

4.1.4 Analysis and design of the buildings

The structural analysis and design software SAP2000 is used for designing the buildings. The buildings are assumed to be fixed at the base in this step. Two types of soils are

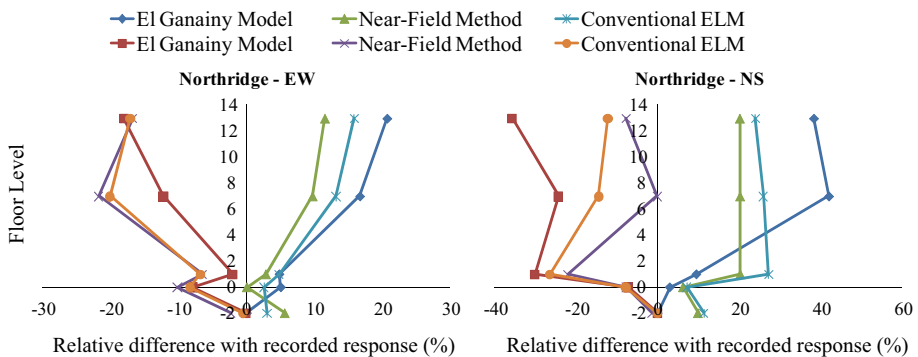


Fig. 4 Relative difference of the near-field, conventional ELM and El Ganainy’s results with the recorded response, Northridge event

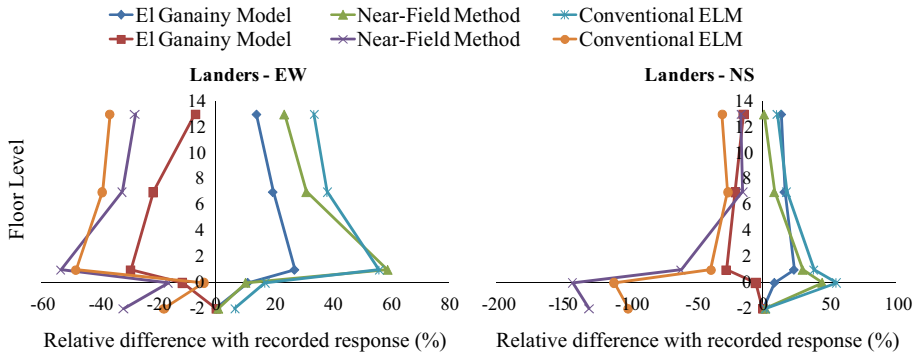


Fig. 5 Relative difference of the near-field, conventional ELM and El Ganainy’s results with the recorded response, Landers event

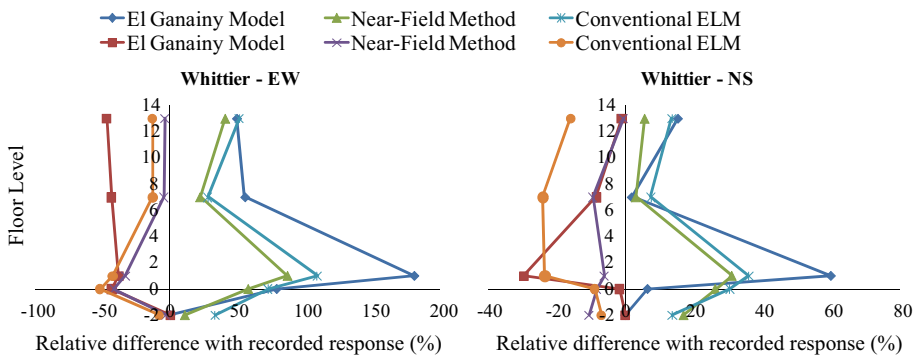


Fig. 6 Relative difference of the near-field, conventional ELM and El Ganainy’s results with the recorded response, Whittier event

considered for design purposes, including the site classes C and E ASCE/SEI 7-10 (2010). The seismic loading is determined using the regulations of ASCE/SEI 7-10 (2010). Table 10 presents the parameters used for the seismic design of the buildings. The structural members are designed according to ANSI/AISC 360-10 (2010) and ANSI/AISC 341-10 (2010). Table 11 lists the design sections for the beams and columns of the steel frames. The fundamental periods of the designed buildings turn out to be 0.79, 1.55, 2.25, and 2.70 s for the 5, 10, 15, and 20-story buildings, respectively.

Mat foundations are designed for all of the buildings. With the allowable bearing capacity being 400 and 150 kPa for the soil types C and E, respectively, thicknesses of the

Table 7 The unit weights and the super-imposed loads

Unite weights (kN/m ³)		Uniformly distributed loads (kN/m ²)	
Steel	77	Nonstructural components	1.1
Concrete	25	Live load	2.4

foundations are proved to be 0.5, 0.75, 1.0 and 1.25 m for 5, 10, 15 and 20 story buildings, respectively.

4.1.5 Nonlinear modeling of the structural members

Concentrated plastic hinges are assigned to the structural members in order to model their nonlinear behavior. The moment-rotation behavior of plastic hinges is introduced according to ASCE 41-13 (2013). Figure 7 illustrates an example of the plastic hinges. In the Fig. 7, values on the horizontal and vertical axes are normalized by the yield deformation and bending capacity of the section, respectively.

4.2 Considered sites

Two soil profiles corresponding to the site classes C and E according to the site classification of ASCE 7-10 (2010) with a total thickness of 30 m on the bedrock are assumed for the buildings sites. Table 12 represents the properties used for modeling the sites selected from ranges specified by ASCE 7-10 (2010) and Das (1999).

4.3 Soil–structure interaction models

The following four different base conditions were assumed in this part of study for evaluating performance of the near-field method:

Table 8 Steel properties

Property	Value
Steel type	ASTM. A992
Modulus of elasticity (GPa)	2
Poisson ratio	0.3
Minimum yield stress (kPa)	344,738
Minimum tensile strength (kPa)	448,159
Effective yield stress (kPa)	379,212
Effective tensile strength (kPa)	492,975

Table 9 Concrete properties

Property	Value
Modulus of elasticity (MPa)	33,000
Poisson's ratio	0.2
Compressive strength (MPa)	30

Table 10 Seismic loading parameters of the buildings ASCE/SEI 7-10 (2010)

S_S (g)	S_1 (g)	F_a	F_v	Importance Factor, I	Response modification factor, R	Deflection amplification factor, C_d
1.919	0.689	1.0 for site class C 0.9 for site class E	1.3 for site class C 2.4 for site class E	1.0	8.0	5.5

Table 11 Designed sections for the beams and columns

Building	Column section	Beam section
5 story	Box 360X25	W24X84
10 story	Box 400X25 and Box 360X25	W24X84
15 story	Box 400X30 and Box 360X25	W24X84
20 story	Box 450X30 and Box 400X25	W24X104

1. Building model with no SSI (the fixed-base model);
2. Soil–structure interaction model utilizing the nonlinear Winkler model proposed by El Ganainy and El Naggar (2009) (El Ganainy’s model);
3. Soil–structure interaction model using the near-field method presented in this study (the near-field model);
4. Soil–structure interaction model using Pressure Dependent Multi-Yield (PDMY) elastic–plastic constitutive model developed by Yang et al. (2003) (the plastic model).

The plastic model is considered as a rigorous model and used as a basis of comparison of results of different models. This model is described in the companion paper. Details of El Ganainy’s model are presented in Sect. 2.1.

4.4 Employing the near-field method

The near-field method is implemented similar to what is explained in example 1. Then height of the near-field zone turns out to be 9 m for all of the models. Length of the near-field zone and properties of the soil in the same region are presented in Table 13.

4.5 Ground motions

Ten consistent ground motions are selected for each of the site classes from the PEER Strong Motion database (2010) and the European Strong Motion Database (2012) with the criteria: $5.5 \leq M \leq 7.5$, $\Delta \geq 15$ km and V_{s30} consistent with each site’s shear wave velocity, with M being the magnitude, Δ the epicentral distance, and V_{s30} the average shear wave velocity in the first 30 m of the soil medium. For scaling of the records the regulations of ASCE 7-10 (2010) are used. The design spectra assumed for the sites are shown in Fig. 8. Characteristics of the selected ground motions for each site are summarized in

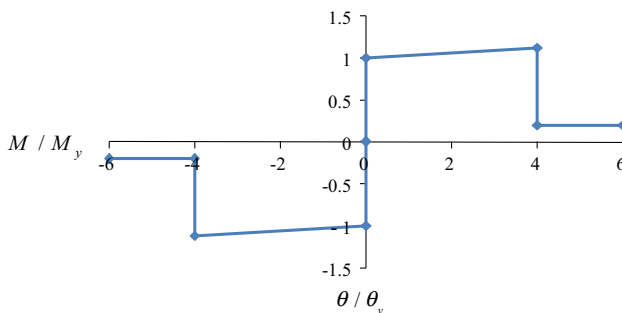


Fig. 7 An example of the plastic hinges (ASCE 41-13 2013)

Table 12 Soil properties selected for site classes C and E

Property	Site class C	Site class E
Shear wave velocity, V_s (m/s)	500	150
Dry unit weight, γ_d (kN/m ³)	20	17
Angle of internal friction, ϕ°	40	30
Poisson’s ratio, ν	0.35	0.35

Table 14. A deconvolution analysis is performed to calculate the ground motion at the bedrock level to be used for SSI analysis with the near-field and plastic models. Shake91 software (Schnabel et al. 1972) is used for the same purpose.

4.6 Analysis steps and the solution procedure

The meshing of the soil medium for the rigorous analysis, the boundary conditions, and selection of the time step in the numerical analysis are explained in the companion paper.

4.7 Nonlinear time history analyses results

As mentioned above, four buildings, two site classes and four modeling procedures are considered herein. Each one of these 32 computational cases is excited by 10 different ground motions and the average of maximum responses is considered as the representative response of the case. Since the main objective of this example is to investigate the performance and accuracy of the near-field method—and not the building response—and because of the extensive amount of results, only some representative results are presented here. The dynamic responses of the structures are presented as maximum displacement, drift ratio and story shear profiles. In addition, the root-mean-square error (RMSE) is calculated for each case to evaluate the accuracy of the modeling technique. The RMSE can be calculated using Eq. 6:

$$RMSE (\%) = 100 \times \sqrt{\frac{\sum_{i=1}^n \left(\frac{X_{Ri} - X_{Ai}}{X_{Ri}} \right)^2}{n}} \tag{6}$$

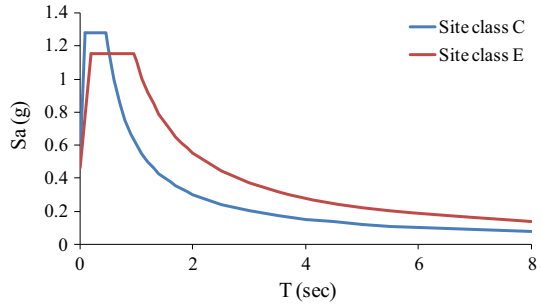
where X_R is the maximum response by the rigorous model, X_A is the maximum response of one another model, both averaged between ten earthquakes, and n is the number of stories.

4.7.1 Lateral displacements

Figure 9 illustrate the averaged maximum lateral displacement profiles of the 20-story building. According to these figures, as is well known, SSI generally increases the lateral

Table 13 Shear modulus reduction factors and damping ratios of the near-field zone in example 2

Building model	5-story on site E	5-story on site C	10-story on site E	10-story on site C	15-story on site E	15-story on site C	20-story on site E	20-story on site C
$L_{N.F.}$ (m)	66	53	64	51	63	50	63	50
$G/G_{Free-Field}$	0.46	0.80	0.48	0.81	0.50	0.82	0.51	0.82
ξ (%)	13.0	4.4	11.5	4.1	10.5	4.0	10.0	4.0

Fig. 8 The design spectra for the site classes E and C**Table 14** Selected ground motions for each site

Number	Event	Station	Magnitude	PGA (g)
(a) Site class C				
1	Cape Mendocino	Shelter Cove Airport	7.01	0.189
2	Coalinga	Slack Canyon	6.36	0.166
3	Duzce	LDEO Station	7.2	0.515
4	Loma Prieta	SF-Presidio	6.93	0.2
5	Northridge	Beverly Hills-12520 Mulh	6.69	0.617
6	Northridge	Rancho Palos Verdes	6.69	0.167
7	Northridge	Sim Valley-Katherine	6.69	0.878
8	Parkfield	Temblor	6.19	0.272
9	San Fernando	Santa Anita Dam	6.61	0.212
10	San Salvador	Geotech Investig Center	5.8	0.475
(b) Site class E				
1	Bucharest	Building Research Institute	7.5	0.201
2	Coalinga	Parkfield-Cholame 2WA	6.36	0.109
3	Imperial Valley	EC Meloland Overpass FF	6.53	0.314
4	Loma Prieta	APEEL2-Redwood City	6.93	0.274
5	Loma Prieta	Larkspur Ferry Terminal	6.93	0.137
6	Montenegro	Veliki Ston	6.9	0.267
7	Superstition Hills	Imperial Valley Wildlife	6.7	0.201
8	Superstition Hills	Salton Sea Wildlife Refuge	6.7	0.167
9	Westmorland	Westmorland Fire Station	5.9	0.368
10	Whittier Narrows	Carson-Water	5.99	0.133

displacements and the effects of SSI are more significant for softer sites where the taller buildings response are more affected. It can be seen that for the site class C the results of the SSI models utilized here are less deviated from the rigorous model. Also, the near-field proves to be more accurate than El Ganainy and fixed-base models.

The RMSE's for the maximum displacements of the buildings are calculated using Eq. 6. Figure 10 shows the RMSE diagrams for various SSI modeling techniques applied to the 20-story building and Table 15 summarizes the RMSE values for the other considered buildings. It is clear from this figure that the cases selected above have been

appropriate for SSI analysis and ignoring SSI in these cases result in considerable errors. The largest error associated with overlooking SSI belongs to the taller buildings on the site class E. On the other hand, the near-field method is proved to be the most accurate one among the others. Furthermore, El-Ganainy’s model seems to have no stable performance as its RMSE in different cases are smaller or larger than those of the fixed-base models.

4.7.2 Drift ratio

Drift ratio profiles of the 20-story building are presented in Fig. 11. The trend of inter-story drift is almost the same for all of the employed SSI models except for two cases of El Ganainy’s model. These figures indicate that SSI can increase inter-story drifts in the lower to middle stories. Increase in the inter-story drift is more pronounced for the site class E. The drift ratios for upper floors of the buildings are almost the same among the cases and in other words, the effect of SSI on the drifts of the upper floors is negligible. Results of the near-field analysis have a better similarity to the rigorous model in most cases. This fact is numerically discussed in the following.

Figure 12 shows the RMSE’s of the drift ratios for the 20-story building estimated by different SSI models. Table 16 lists the RMSE’s of the drift ratios for other cases. As observed, the near-field method exhibits the least error for all of the cases considered. Again, the El Ganainy’s method shows an unstable performance similar to what is mentioned for lateral displacements.

4.7.3 Story shear

Story shear envelopes of the 20-story building are illustrated in Fig. 13. The envelopes show similar trends and make a well known fact revisited that SSI reduces the story shears. Inspecting the whole set of graphs shows that the reduction in story shear is larger for lower stories, taller buildings, and softer soil conditions and is negligible for upper stories of the taller buildings. In addition, the base shear, i.e. the story shear at the first story, obtained from the rigorous model is from 7 to 28 % smaller than that of the fixed-base model and for all of the cases except for the 5-story building on the site class E, the near-field method gives a better estimation of the story shears with a slight overestimation.

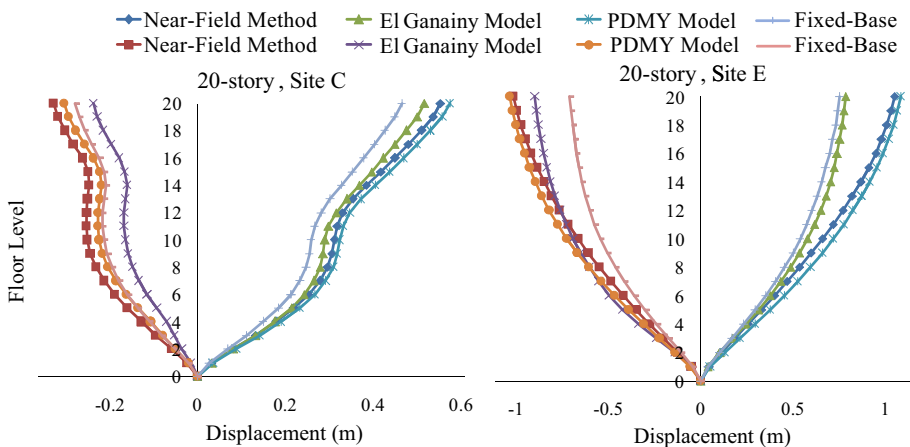


Fig. 9 Averaged maximum displacement profiles for 20-story building

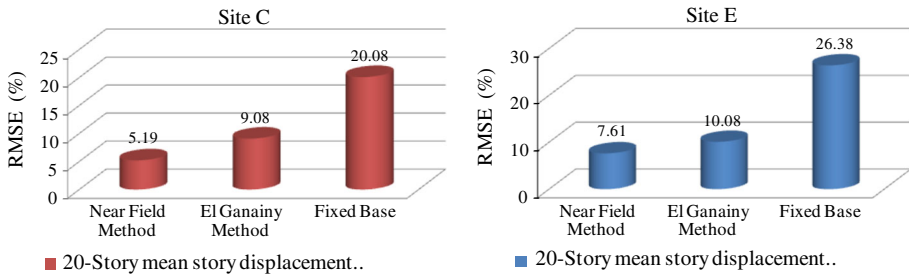


Fig. 10 RMSE's for the averaged maximum displacements of 20-story building (see Eq. 6)

Table 15 RMSE's for the averaged maximum displacements of 5, 10 and 15-story buildings

Building	Site class	SSI modeling technique	RMSE (%)
5-story	Site C	Near-field method	3.44
		El Ganainy method	7.90
		Fixed-base	8.91
	Site E	Near-field method	12.12
		El Ganainy method	23.39
		fixed-base	14.56
10-story	Site C	Near-field method	4.37
		El Ganainy method	15.12
		Fixed-base	20.15
	Site E	Near-field method	3.55
		El Ganainy method	4.64
		Fixed-base	19.04
15-story	Site C	Near-field method	6.06
		El Ganainy method	18.65
		Fixed-base	14.98
	Site E	Near-field method	8.43
		El Ganainy method	17.98
		Fixed-base	25.87

Diagrams and values of the story shear RSME's are presented in Fig. 14 and Table 17, respectively. Again the near-field method shows the maximum accuracy with RMSE's less than 10 % for all of the cases. Similar to the previous responses, the El Ganainy's model shows an unstable behavior with estimating responses larger or smaller than the fixed-base ones as before. Errors arising from neglecting SSI are larger for taller buildings on the softer soil and vary between 14–30 and 19–35 % for the site classes C and E, respectively.

5 Conclusions

The near-field method, as a procedure for simplifying the direct analysis of SSI problems taking into account soil nonlinearity especially in the vicinity of foundations, was introduced in a companion paper. This method proposes semi-analytical equations for

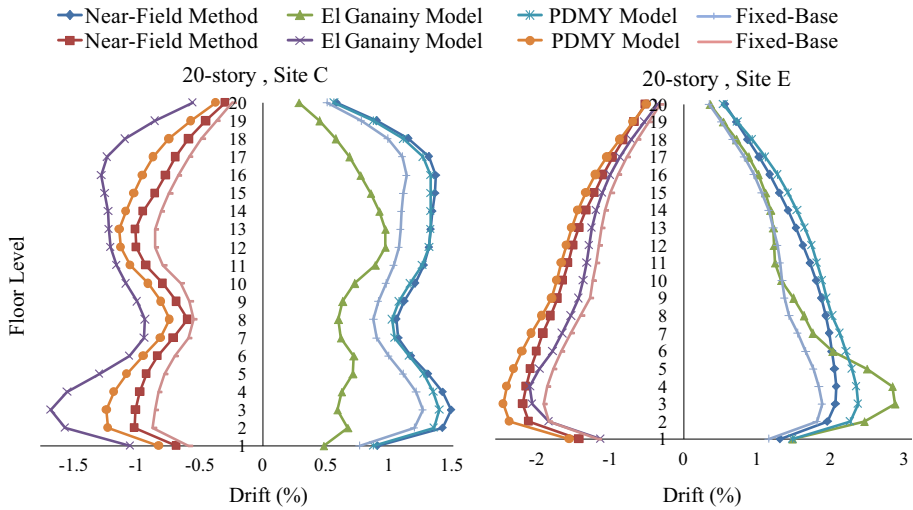


Fig. 11 Averaged maximum drift ratio profiles for the 20-story building

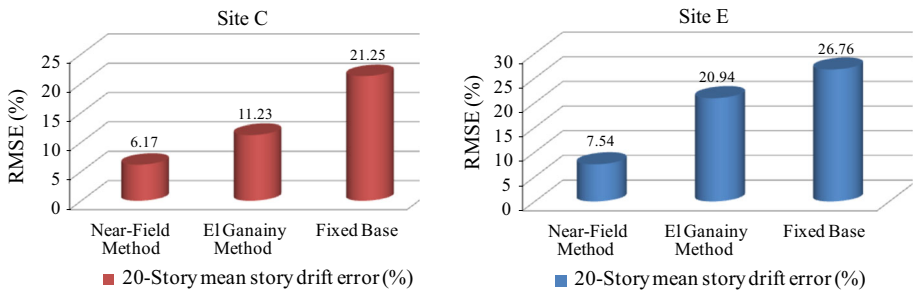


Fig. 12 RMSE's for the drift ratios of the 20-story building

modifying properties of the linear soil in the near field of foundations as well as the near-field dimensions.

Evaluation of the accuracy of the near-field method was the main goal of this research. Accordingly, two examples were considered to introduce steps of employing the near-field method and to investigate its accuracy and performance.

An existing building (Sherman Oaks building) was selected as the first example and its recorded maximum responses during recent earthquakes were utilized as the basis of comparison. In the second example, four buildings having 5, 10, 15, and 20 stories with 3D steel moment-resisting frames were designed for the purposes of this study. Two site conditions corresponding to the site classes C and E were considered. Each model was excited by ten different ground motions and the maximum responses were averaged among the ground motions to be compared between the methods. Accuracy of the near-field method to estimate different responses of nonlinear buildings resting on nonlinear soils was compared in the above examples with another method comprising of nonlinear Winkler springs at the base of columns (2009).

Table 16 RMSE's for the drift ratios of 5, 10 and 15-story buildings

Building	Site class	SSI modeling technique	RMSE (%)
5-story	Site C	Near-field method	5.45
		El Ganainy method	10.71
		Fixed-base	9.27
	Site E	Near-field method	10.16
		El Ganainy method	22.69
		Fixed-base	17.13
10-story	Site C	Near-field method	5.98
		El Ganainy method	11.94
		Fixed-base	19.07
	Site E	Near-field method	4.74
		El Ganainy method	8.18
		Fixed-base	18.39
15-story	Site C	Near-field method	5.77
		El Ganainy method	15.19
		Fixed-base	13.82
	Site E	Near-field method	12.19
		El Ganainy method	15.05
		Fixed-base	21.90

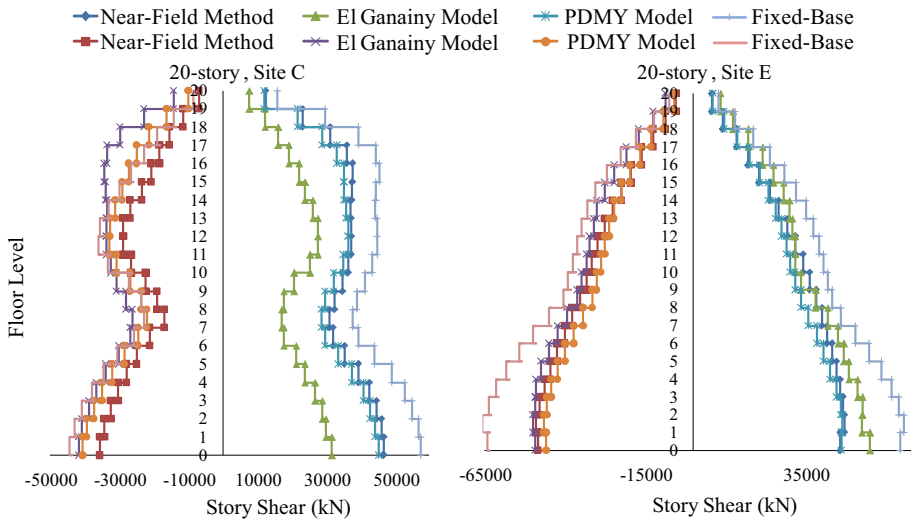


Fig. 13 Story shear envelopes for the 20-story building

Through computation of root-mean-squares of errors with respect to the recorded data in the first example and plastic modeling of soil in the second example, it was shown that almost in all of the cases the near-field method possesses a superior accuracy. Regarding the time of computation, when for a sample case dynamic analysis of the SSI system with a nonlinear structure and a plastic soil takes about 4 h, analyzing the same system with the

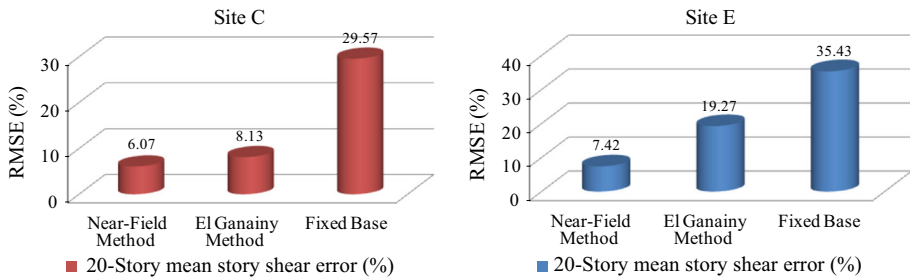


Fig. 14 RMSE's for the story shears of the 20-story building

Table 17 RMSE's for the story shears of 5, 10 and 15-story buildings

Building	Site class	SSI modeling technique	RMSE (%)
5-story	Site C	Near-field method	5.65
		El Ganainy method	18.15
		Fixed-base	13.84
	Site E	Near-field method	8.50
		El Ganainy method	26.23
		Fixed-base	18.91
10-story	Site C	Near-field method	8.73
		El Ganainy method	17.70
		Fixed-base	27.01
	Site E	Near-field method	9.07
		El Ganainy Method	15.80
		Fixed-base	32.20
15-story	Site C	Near-field method	8.58
		El Ganainy method	30.89
		Fixed-base	26.06
	Site E	Near-field method	7.58
		El Ganainy method	18.99
		Fixed-base	25.81

near-field method, including the time needed for calculation of the modified parameters, takes only 20 min. Therefore, the near-field method can be an efficient alternative for dynamic analysis of nonlinear soil-structure systems.

References

ANSI/AISC 341-10 (2010) Seismic provisions for structural steel buildings. American Institute of Steel Construction, Chicago
 ANSI/AISC 360-10 (2010) Specification for structural steel buildings. American Institute of Steel Construction, Chicago
 ASCE 41-13 (2014) Seismic evaluation and retrofit of existing buildings. American Society of Civil Engineers (ASCE), Virginia

- ASCE/SEI 7-10 (2010) Minimum design loads for buildings and other structures. American Society of Civil Engineers (ASCE), Virginia
- Bozorgnia Y, Bertero VV (2004) Earthquake engineering from engineering seismology to performance-based engineering. CRC Press, New York
- Casciati S, Borja RI (2004) Dynamic FE analysis of South Memnon Colossus including 3D soil–foundation–structure interaction. *Comput Struct* 82(20):1719–1736
- Chen X, Birk C, Song C (2015) Transient analysis of wave propagation in layered soil by using the scaled boundary finite element method. *Comput Geotech* 63:1–12
- Cubrinovski M, Ishihara K (2004) Simplified method for analysis of piles undergoing lateral spreading in liquefied soils. *Soils Found* 44(5):119–133
- Das BM (1999) Fundamentals of geotechnical engineering. Brooks/Cole, Pacific Grove
- El Ganainy H, El Naggar MH (2009) Efficient 3D nonlinear Winkler model for shallow foundations. *Soil Dyn Earthq Eng* 29(8):1236–1248
- Ghandil M, Behnamfar F (2015) The near-field method for dynamic analysis of structures on soft soils including inelastic soil–structure interaction. *Soil Dyn Earthq Eng* 75:1–17
- Ishihara K (1996) Soil behaviour in earthquake geotechnics. Clarendon Press, Oxford
- Manna B, Baidya DK (2010) Dynamic nonlinear response of pile foundations under vertical vibration—theory versus experiment. *Soil Dyn Earthq Eng* 30(6):456–469
- Mazzoni S, McKenna F, Scott MH, Fenves GL, Jeremic B (2007) OpenSees command language manual. Pacific Earthquake Engineering Research Center, University of California at Berkeley, Berkeley
- Mckenna FT (1997) Object-oriented finite element programming: frameworks for analysis, algorithms and parallel computing. Ph.D. Dissertation, University of California Berkeley
- National Institute of Standards and Technology (2012) NIST GCR 12-917-21 (ATC-83): soil–structure interaction for building structures. NEHRP Consultants Joint Venture
- PEER Strong Motion Database (2010). <http://peer.berkeley.edu/smcat/>
- Pitilakis D, Clouteau D (2010) Equivalent linear substructure approximation of soil–foundation–structure interaction: model presentation and validation. *Bull Earthq Eng* 8(2):257–282
- Schnabel PB, Lysmer J, Seed HB (1972) SHAKE-A computer program for response analysis of horizontally layered sites. Report No. EERC 72-12. University of California, Berkeley, CA
- The European Strong-Motion Database (2012). <http://www.isesd.hi.is/ESD> Local/frameset.htm
- Wolf JP, Song C (1996) Finite-element modelling of unbounded media. Wiley, Chichester
- Yang Z, Elgamal A, Parra E (2003) Computational model for cyclic mobility and associated shear deformation. *J Geotech Geoenviron Eng* 129(12):1119–1127